Total cross sections for charge transfer for F^+ in H_2, N_2, He, Ne, and Ar†

G. J. Lockwood
Sandia Laboratories, Albuquerque, New Mexico 87115
(Received 12 November 1973)

Absolute measurements are reported of the total cross section σ_{10} for charge transfer of F^+ in H_2, N_2, He, Ne, and Ar in the energy range from 14 to 100 keV. The measured cross sections are in qualitative agreement with theory. However, it is observed that the slopes of the cross section versus velocity for velocities above the maximum in the cross sections differ for molecular and atomic targets used in this study.

INTRODUCTION

Total cross sections are reported here for charge transfer when energetic fluorine ions are incident on H_2, N_2, He, Ne, and Ar gas. The energy range covered was 14–100 keV. Interest in F^+ as an incident ion was stimulated by the relatively small energy defect (–1.4 eV) for the process

$$F^+(^3P) + N_2(X^1\Sigma) \rightarrow F(^2P) + N_2^+(B^2\Sigma), \quad (1)$$

i.e., charge transfer with the target ion left in an excited state. The emission cross section at 3914 Å resulting from this excited state of N_2^+ will be published as a separate paper.

Charge transfer of F^+ in N_2 leading to the ground state of N_2^+ has an energy defect of +1.9 eV, which nearly equals the energy defects of +1.8 and +1.7 eV for charge transfer of F^+ in H_2 and Ar, respectively. Thus the measurements were extended to include targets of H_2 and Ar to examine the dependence of the charge-transfer cross section on target structure where the energy defect is nearly the same. Targets of He and Ne were included with the Ar to examine the dependence of the cross section on energy defect for targets that are similar in the fact that they are all noble gases.

APPARATUS AND EXPERIMENTAL PROCEDURES

Sandia Laboratories 100-kV ion accelerator was used in this study. The ions were produced in an rf ion source using BF_3 and SF_6 gas. The use of an rf source was necessary to obtain beams with sufficient intensity to make the emission cross-section measurements with the available apparatus. Since this is an energetic source, there is a possibility of excited (metastable) state ions being in the beam.[1] The metastable levels of F^+ are at 2.6 and 5.6 eV above the ground state of F^+. It seems unlikely that the equilibrium distribution of excited states would be the same in the plasmas resulting from the two different source gases, and cross sections measured with F^+ ions at various energies were independent of the source gas used. Therefore, it appears that a large metastable population in the F^+ ion beam was not a problem. The accelerator delivered a beam of magnetically analyzed ions having small energy spread (less than 35 eV) to the experimental chamber. The beam energy was determined to 2.0% by measuring the terminal potential with a voltage divider and correcting for ion-source potentials.

The experimental apparatus (Fig. 1), procedures, and data reduction used in this study have been described in detail in earlier papers,[1–3] so only a brief description will be given here. The incident ion beam, collimated to ±0.10° by apertures *A* and *B*, enters the collision chamber through *B*. After traversing 1.6 cm of target gas, the beam exits the collision chamber through aperture *C*. Apertures *C* and *D* are used to collimate the scattered ion beam and allow all particles which have scattered into a cone of half-angle 1.0° to reach the detector. This acceptance angle ensures that no scattered particles hit the analyzer plates between aperture *D* and the detector. The detector is a secondary electron multiplier (SEM). The first dynode of the SEM is maintained at ground potential so that all particles strike the first dynode with the same energy except for small collisional losses. To a good approximation[4,5] the output of the SEM is independent of the particle charge.

The cross sections are obtained from the equation

$$\sigma_{10} = (I_0/I_1)/(3.54\times10^{16} P l \times 273/T), \quad (2)$$

where I_1 is the SEM current when the incident ion beam was allowed to strike the first dynode, and I_0 is the SEM current when all charged particles in the scattered beam were swept away by the electrostatic analyzer and only the neutral component reached the detector. P is the pressure in Torr and l is the thickness of target gas in the direction

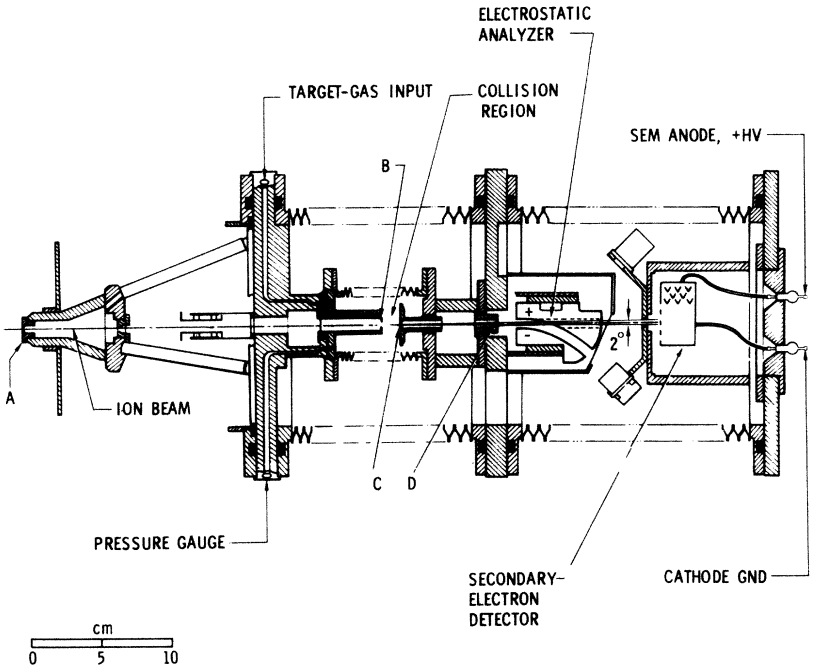

FIG. 1. Experimental apparatus.

of the beam. To within 1%, l is the measured distance (1.6 cm) between holes B and C.[2] The ratio I_0/I_1 is equal to $N_0\gamma_0/N_1\gamma_1$, to within the approximation that the SEM output is independent of particle charge, $\gamma_0 = \gamma_1$ and $I_0/I_1 = N_0/N_1$. The constant 3.54×10^{16} is the number of particles per Torr cm^3 at 273 °K and T is the chamber temperature.

In the procedure used, the ratio I_0/I_1 was obtained for at least ten different pressures in the range from 1×10^{-4} to 10×10^{-4} Torr at each energy. A plot of I_0/I_1 versus pressure was made from the data, and the cross section was determined from the slope of the line obtained by a least-squares fit to the data. Figure 2 is a typical data curve of this type.

The angular distribution of scattered particles was examined. The results indicated that neutral particles which scatter into a cone of half-angle 1.0° constitute greater than 95% of the total scattered neutrals.

The experimental uncertainty in σ_{10} is ±9% and was obtained by considering the sources and esti-

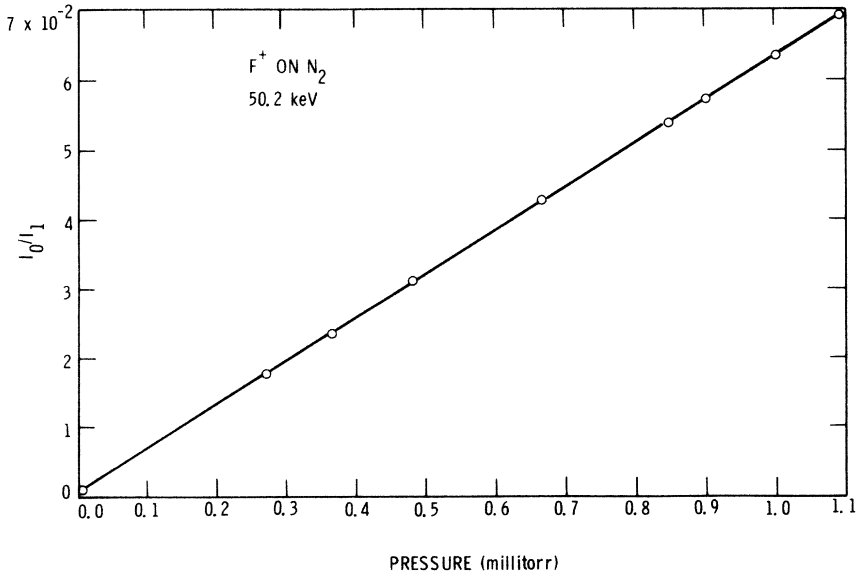

FIG. 2. Ratio of current associated with neutral particles to current associated with the incident ion beam vs target gas pressure. The slope of the line which was obtained by a least-squares fit to the data is used in determining the σ_{10} cross section.

TABLE I. Sources and estimated uncertainties leading to the experimental uncertainty of ±9% in σ_{10}.

Source	Sources and estimated uncertainty (%)	Uncertainties, remarks
Target thickness l	1	See discussion Sec. II, Ref. 2
Incident current reading I_1	3	Electrometer limitation
Neutral current reading I_0	3	Electrometer limitation
γ cancellation in ratio I_0/I_1	5	Based on laboratory studies
Pressure	2	Maximum estimated error due to scale factor. This is conservative, based on manufacturer's specifications.
Small-angle scattering	5	Based on laboratory measurements

mated uncertainties listed in Table I. Other potential sources of error (i.e., residual gas scattering, capture in the accelerator tube, and target gas impurities) have been reduced to < 1% by either experimental arrangement or data acquisition and reduction procedures.

DATA AND DISCUSSION

Data from the present study are shown in Fig. 3 and tabulated in Table II.

The general shapes of the curves of cross section versus velocity can be compared with the predictions of the adiabatic criterion. The adiabatic criterion predicts, that for charge transfer between unlike particles the cross section should be small at low velocity, rise to a maximum, and fall as the velocity is increased. The velocity v_m at which the maximum occurs is found to be proportional to the internal energy defect ΔE and is given by $v_m = \alpha|\Delta E|/h$, where h is Planck's constant and α is a length of atomic dimensions. Analysis of a large number of experimentally determined cross sections yields a value of 7 Å (Ref. 6) for the length α when the ΔE is taken as the energy defect of ground-state to ground-state transfer. Using these arguments the velocity corresponding to the maximum in the cross sections measured in the present study can be predicted. For targets of Ar, N_2, and H_2 the maximum in the cross section versus velocity is predicted to be at a velocity below the lowest velocity reached in this experiment. Thus the cross sections would be expected to rise as the velocity is decreased, which is the case as seen in Fig. 3. For a Ne target a maximum is predicted at about 7×10^7 cm/sec for ground-state to ground-state charge transfer. The

TABLE II. Cross sections for charge transfer of F^+ on H_2, N_2, He, Ne, and Ar. Experimental uncertainty in σ_{10} is 9%.

Velocity (10^7 cm/sec)	σ_{10} (10^{-16} cm^2)	Velocity (10^7 cm/sec)	σ_{10} (10^{-16} cm^2)
H_2		He	
3.73	8.95	3.76	0.860
4.47	8.35	4.47	1.29
5.02	7.84	5.60	1.97
5.52	7.23	6.36	2.38
6.39	6.68	7.13	2.96
7.10	6.63	7.78	3.21
7.81	5.79	8.43	3.39
8.45	5.56	9.00	3.52
9.02	4.82		
N_2		Ne	
3.90	17.3	3.77	5.45
3.90	17.2	4.49	6.54
4.49	16.1	5.02	6.57
4.49	15.2	5.54	6.78
5.03	15.0	6.36	6.47
5.06	14.8	7.14	6.44
5.51	14.0	7.80	6.24
5.52	14.0	8.45	6.16
6.36	12.4	9.00	5.83
6.38	12.8	10.1	5.40
7.14	11.7	Ar	
7.17	10.6	3.74	13.6
7.83	10.6	4.51	13.4
7.84	10.3	5.08	12.9
8.48	9.50	5.53	12.3
9.07	9.12	6.35	11.4
10.0	8.11	7.14	11.4
		7.78	10.7
		8.44	10.4
		9.03	9.98
		10.1	9.45

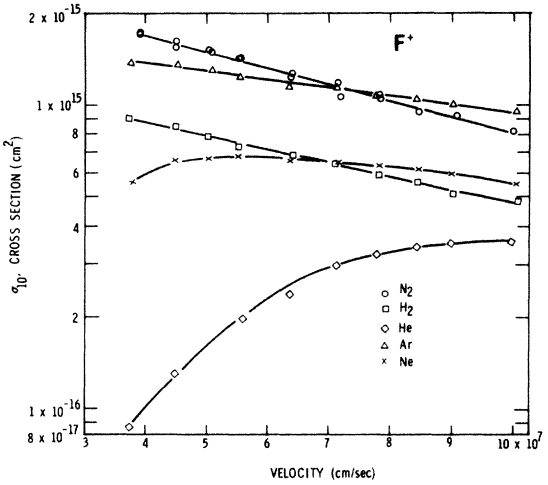

FIG. 3. Total cross section for charge transfer σ_{10} of F^+ on H_2, N_2, He, Ne, and Ar vs velocity of the incident F^+.

Ne curve in Fig. 3 shows a broad maximum in the vicinity of 7×10^7 cm/sec. The adiabatic maximum for a He target is predicted to be at 12×10^7 cm/sec which is above the maximum velocity reached in this experiment. Thus, the F^+ on He data would be expected to be rising as the velocity is increased. This agrees with the data for the He target shown in Fig. 3. All the data presented here agree generally with the adiabatic theory for ground-state to ground-state charge transfer. However, additional comparisons can be made for the four target gases for which the data extend beyond the adiabatic maximum. It is seen that the N_2 and H_2 data have the same slope and that the Ne and Ar data also have the same slope but different from N_2 and H_2. In both cases the target with more electrons had the larger cross section at a given velocity, as would be expected. This behavior of the Ne and Ar data is in qualitative agreement with theory and other ion-atom charge-transfer measurements.[6] The theory predicts that for ion velocities greater than that of the maximum cross section, the unlike ion-atom charge-transfer function and that for a symmetrical resonance process have the same form. Measurements with other ion-atom combinations show that the shapes in cross section versus velocity for a common ion with various atomic targets are nearly the same at high velocity, although the magnitudes of the cross sections are not necessarily equal.[6] However, it is obvious that the shapes obtained from the present data for molecular and atomic targets differ. Due to this difference in shape, the cross section for Ar falls below that of N_2 at low velocity. Unfortunately, there is no theory at present that will accurately predict the shapes of these heavy-particle cross sections to the point that the difference in shape between the data for atomic and molecular targets can be understood.

ACKNOWLEDGMENTS

The author gratefully acknowledges the assistance of L. E. Ruggles in collecting the data and Dr. G. H. Miller for valuable discussions held during this study.

†This work was supported by the United States Atomic Energy Commission.

[1]G. J. Lockwood, Phys. Rev. A 2, 1406 (1970).
[2]G. J. Lockwood, Phys. Rev. 187, 161 (1969).
[3]G. J. Lockwood, Phys. Rev. A 7, 125 (1973).
[4]A. H. J. Boerbroom, B. L. Schram, W. Kleine, and J. Kistermaker, Z. Naturforsch. A 21, 127 (1966).
[5]Unpublished study of charge-state dependence conducted by author.
[6]J. B. Hasted, *Physics of Atomic Collisions* (Butterworths, London, 1964), Chap. 12.